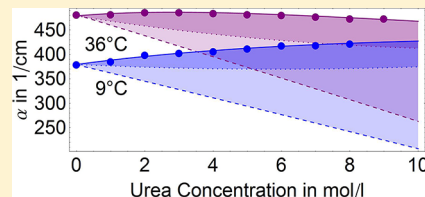


# Urea, a Structure Breaker? Answers from THz Absorption Spectroscopy

Stefan Funkner, Martina Havenith, and Gerhard Schwaab\*

Department of Physical Chemistry II, Ruhr-University Bochum, Germany

**ABSTRACT:** There has been a controversial debate of whether urea can be regarded as structure breaker or a structure maker. Here, we present concentration and temperature dependent absorption coefficients of urea–water mixtures in the THz range (1.5–10 THz, 50–350  $\text{cm}^{-1}$ ). Our results are in agreement with the hypothesis that urea adapts ideally into the water network. Using a semi-ideal chemical association model and accompanying MD simulations, the observed spectra could be decomposed in three contributions: one is attributed to bulk water, a second one to rattling modes of weakly solvated urea in the surrounding water cage, and the third part accounts for THz modes describing a doubly hydrogen bonded strong solvent–solute interaction. The bands attributed to the rattling motion of the solute scale linearly with concentration. The intensity of this contribution is temperature independent in contrast to the water and strongly solvated solute absorption. We find that even at high urea concentrations the majority of water retains a bulklike absorption spectrum, whereas only a small number (about 0.5–1.1 per urea on average) are strongly bound in the temperature range between 9 and 36 °C. The THz absorption data provide no evidence for urea aggregation in the concentration range investigated (1–10 M).



## INTRODUCTION

Urea serves as a well-known denaturant for proteins. Surprisingly, the underlying molecular mechanism, which drives denaturation is still part of an ongoing debate. Different mechanisms have been discussed in the literature: Initially, urea was proposed to be structure breaker of the water hydrogen bond network<sup>1</sup> causing an increased solvation of hydrophobic groups.<sup>2</sup> These ideas have been supported by NMR measurements,<sup>3</sup> Raman spectra,<sup>4,5</sup> molecular dynamics (MD) simulations,<sup>6</sup> and by viscosity measurements of aqueous urea mixtures.<sup>7,8</sup>

However, more recent pump–probe IR-measurements,<sup>9</sup> NMR,<sup>10</sup> and neutron diffraction studies<sup>11</sup> questioned the structure breaking hypothesis. MD simulations by Hua et al.<sup>12</sup> showed that, for hen lysozyme, urea unfolds the protein in a 2-stage process. In a first step, water is excluded from the protein solvation shell by direct binding of urea. This is causing a swelling of the lysozyme. In a second step, urea and water will solvate the protein interior. The preferential binding of urea to the hydrophobic parts of protein was suggested to lead to a dewetting and weakening of the hydrophobic effect.<sup>13,14</sup>

Stumpe and Grubmüller have studied the influence of solvating with an aqueous urea solvent for the native state and for partially unfolded conformations of the cold shock protein Bc-CsP from *Bacillus caldolyticus*.<sup>15</sup> They concluded that conformational fluctuations of the native state which are reversible in water are rendered irreversible in urea solvents due to favorable interactions with urea molecules. MD simulations of the Trp-cage miniprotein of Canchi et al.<sup>16</sup> propose a preferential binding of urea by dispersion as well as electrostatic forces.

Low frequency bands for solvated urea have been reported using ultrafast Optical Kerr effect spectroscopy by Idrissi et al.<sup>17</sup>

and by Mazur et al.<sup>18</sup> As a result of an analysis of their data, they reported bands at 60  $\text{cm}^{-1}$ , 100  $\text{cm}^{-1}$  and 200  $\text{cm}^{-1}$  and 45  $\text{cm}^{-1}$ , 80  $\text{cm}^{-1}$  and 175  $\text{cm}^{-1}$ , respectively. The low frequency bands around 45–60  $\text{cm}^{-1}$  were assigned to either a low frequency response of a vibration of water or urea in a cage<sup>17</sup> or attributed to absorption of water.<sup>18</sup> The band observed at 150–175  $\text{cm}^{-1}$  or 200  $\text{cm}^{-1}$  is assigned to the low frequency mode of bulk water, which has a well-known absorption centered at 200  $\text{cm}^{-1}$ . The decrease of the peak frequency with increasing urea concentration, as reported in the article by Mazur et al.,<sup>18</sup> is attributed to a distortion of the water network. However, this decrease is not observed in the previous optical Kerr effect measurements. The band around 100  $\text{cm}^{-1}$  is found to be temperature independent.<sup>17</sup> It was attributed to the hydrogen bond interaction of urea with water and to the librational band of urea in the cage. This interpretation agrees with the assignment of Mazur et al.<sup>18</sup> for the band centered around 70–80  $\text{cm}^{-1}$ , the so-called G-mode, which increases linearly with concentration. Similar bands which were assigned to rattling motions of ions in the cage, with even more rigid hydration shells have been observed by us for salts.<sup>19,20</sup>

In the present article, we have focused on the frequency range from 1.5 to 10 THz (50–350  $\text{cm}^{-1}$ ) to study the changes in the fast solvation dynamics in aqueous urea solutions compared to bulk water. As could be shown in our previous paper, THz absorption spectroscopy in this range opens a new window and provides a sensitive tool to probe the subsec collective motions of the water network and the coupled solute/hydration shell.<sup>21,22</sup>

**Received:** September 1, 2012

**Revised:** October 24, 2012

**Published:** October 26, 2012

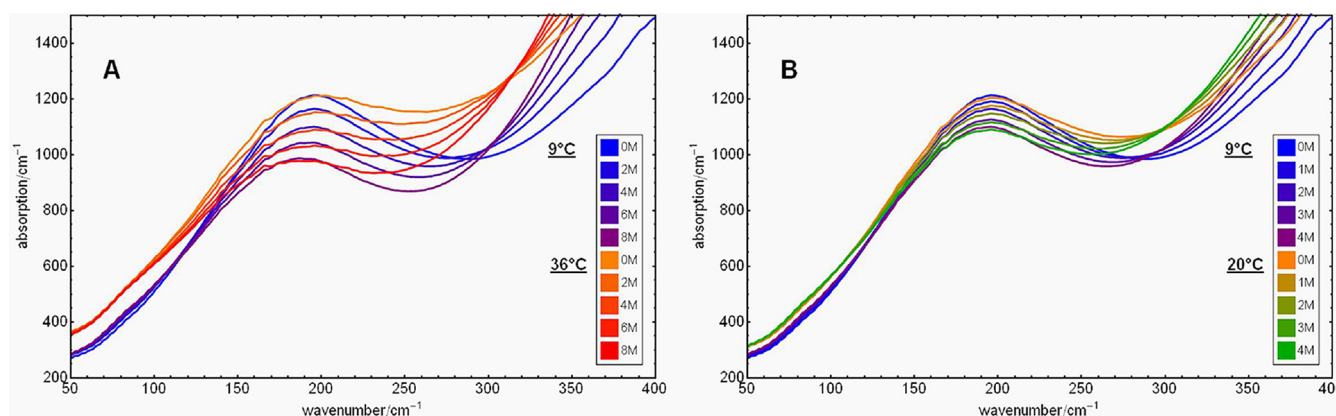


**Figure 1.** Shown is a comparison of the concentration dependent absorption of aqueous urea solutions between (A) 9 and 36 °C and (B) 9 and 20 °C.

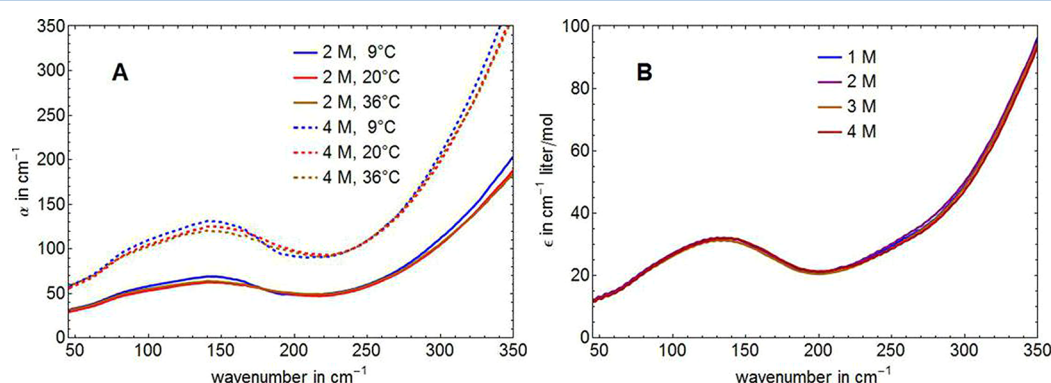


**Figure 2.** (A) Partial THz absorption spectrum for an aqueous urea solution of 2 M (solid line) and 4 M (dashed) at 9, 20, and 36 °C (after subtracting the bulk water contribution). (B) Partial solute THz extinction (at 20 °C).

Using a THz-FT spectrometer, we have recorded overview spectra in the frequency range between 50 and 350  $\text{cm}^{-1}$ . In addition, we have carried out high precision THz absorption measurements around 80  $\text{cm}^{-1}$  using our home-built p-Ge laser difference spectrometer.<sup>23</sup> The bulk water spectrum exhibits two prominent absorption features in this particular frequency region: the tail of a peak extending to frequencies beyond 350  $\text{cm}^{-1}$  and a band with a maximum at  $\sim 200 \text{ cm}^{-1}$ . Both features are well-known<sup>24,25</sup> and are assigned to the hindered libration of water molecules in the hydrogen bond network at 700  $\text{cm}^{-1}$  and to first-shell dynamics of the hydrogen bond stretch modes, respectively.<sup>26</sup> In aqueous urea solution, we report here the observation of two temperature independent absorption bands at  $100.0 \pm 2.2$  and  $153.3 \pm 1.3 \text{ cm}^{-1}$  that are attributed to rattling motions of weakly solvated urea in the surrounding water cage and a strongly solvated urea band at a frequency around 80  $\text{cm}^{-1}$ .

## EXPERIMENTAL AND COMPUTATIONAL RESULTS

**Broadband Fourier Transform Terahertz Spectroscopy.** In Figure 1, we display the FT THz spectra of aqueous urea solutions for different concentrations and temperatures. For most parts of the frequency spectrum, the higher temperature solutions (yellow to red) show an increased absorption compared to lower temperature solutions (blue to purple). We find two isosbestic points in the spectrum: One at ca. 310  $\text{cm}^{-1}$ , which shows a blue shift with increasing temperature and a second between 70  $\text{cm}^{-1}$  and 100  $\text{cm}^{-1}$ , which shows a red shift with increasing temperature. This indicates a mostly ideal

behavior of the solution, that is that the total absorption may be described as a concentration weighted linear superposition of the constituent absorptions.

We determined the partial water concentration from density measurements and subtracted the corresponding bulk water absorption (i.e., the last term in eq 8, as seen in the Methods section). The resulting difference spectra are shown in Figure 2 A. They contain a sum of the partial THz absorption of urea, urea–water clusters, and any changes in the water extinction due to solvation. In contrast to the bulk water spectrum, the difference spectra are nearly independent of temperature. A slight tendency to higher absorption with lower temperature at 150  $\text{cm}^{-1}$  and at 350  $\text{cm}^{-1}$  is observed for both concentrations on display. In part B of Figure 2, the molar extinction of aqueous urea solutions at 20 °C is shown for different concentrations. This partial THz extinction is constant within our experimental uncertainties in the covered concentration range. The same result is obtained at 9 and 36 °C.

Thus, the temperature dependence found in Figure 1 is explained in terms of a linear superposition of temperature independent urea extinction (panel B of Figure 2) and water extinction that increases with temperature over most parts of the frequency range covered.<sup>24</sup> In summary, the temperature dependence of the urea–water mixture absorption can nearly exclusively be attributed to the temperature dependence of the partial bulk water contribution. The difference spectra can be fitted to two separate absorption bands with peak positions at 100 and 153  $\text{cm}^{-1}$ . To describe the low and high frequency tails properly we needed to include two more peaks with band

centers at 36 and 400  $\text{cm}^{-1}$ . The low frequency component is close to the band at 45–60  $\text{cm}^{-1}$  reported previously, and the high frequency tail might be connected to either a water band centered at 400  $\text{cm}^{-1}$ ,<sup>24</sup> or to an intramolecular urea mode. However, because the center frequencies lie outside our observational range they cannot be determined unambiguously and will therefore not be discussed anymore.

**Molecular Dynamics Simulations.** To investigate the origin of the solvated urea bands we performed molecular dynamics (MD) simulations of solvated urea using the program package GROMACS 3.3.<sup>27</sup> On the basis of the trajectories of these simulations we have calculated the mass weighted vibrational density of states (VDOS) for urea molecules using the Fourier transformation of the time autocorrelation function of the atomic velocities  $v_i$ :<sup>28</sup>

$$\text{VDOS}(\omega) = \frac{2}{kT} \sum_{i=1}^N m_i \int_{-\infty}^{\infty} \langle \vec{v}_i(0) \vec{v}_i(t) \rangle e^{i\omega t} dt \quad (1)$$

The result (averaged over 56 urea molecules and 20 trajectories) is shown in Figure 3.

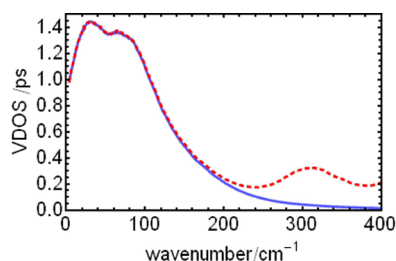


**Figure 3.** Compared are the VDOS of urea in aqueous solution (dashed red line) and the  $\text{VDOS}_{\text{ext}}$  attributed to external degrees of freedom by the urea molecule (solid blue line).

To reveal the nature of the low frequency modes (0–200  $\text{cm}^{-1}$ ), we have separated the motions of urea into its rotational and translational intermolecular network modes and its intramolecular vibrations. For every frame and individual urea in NVE ensemble trajectory, we determined the Eckart frame,<sup>29,30</sup> with the reference structure from Brown et al. and Vijay et al.<sup>31,32</sup> The coordinates of the Eckart frame are chosen to minimize the coupling between rotational and translational motions on the one hand and intramolecular vibrations on the other hand. Hence, the motion of the molecule can be dissected in the translational (center of mass) and rotational (angular motion) velocities of the urea Eckart frame and internal vibrations. We define the sum of the translational and rotational velocity as  $v_{\text{ext}}$ . Finally, we calculate  $\text{VDOS}_{\text{ext}}$  using these external degrees of freedom as the Fourier transformation of the autocorrelation function of  $v_{\text{ext}}$ .

The comparison of the full vibrational density of states to  $\text{VDOS}_{\text{ext}}$  is displayed in Figure 3 and shows that in the frequency range between 0 and 200  $\text{cm}^{-1}$   $\text{VDOS}_{\text{ext}}$  contributes more than 98.8% to the total VDOS and shows two maxima at 30 and 70  $\text{cm}^{-1}$ . The lowest frequency intramolecular mode of urea appears at 300  $\text{cm}^{-1}$ . This demonstrates that the VDOS of urea in the low frequency range is dominated by particle motions corresponding to intermolecular motions.

Furthermore, we have calculated the VDOS of water in the dynamical hydration shell and compared this with the VDOS of bulk water. For the dynamical hydration shell we have considered all water molecules which lie within a distance of

less than 0.5 nm to the atoms of the urea molecule. Only those trajectories were considered which remained longer than 10 psec within the defined dynamical hydration shell or outside this shell (Figure 4).

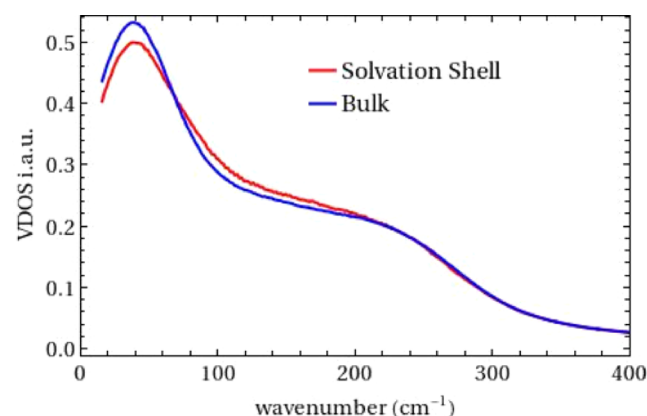


**Figure 4.** Compared are the VDOS of urea in aqueous solution (dashed red line) and the  $\text{VDOS}_{\text{ext}}$  attributed to external degrees of freedom by the urea molecule (solid blue line).

Under the assumption that the emissivity of the solvation shell modes is similar to those of bulk water modes, these calculations indicate a decrease in the absorption coefficient in the dynamical hydration shell for low frequencies and an increase for frequencies above 60  $\text{cm}^{-1}$ . The results indicate a blue shift of the solvated urea modes similar to that found in hydration water around proteins.<sup>26</sup> There we showed that the shift of the peak maximum is connected with retardation in the hydrogen bonds dynamics in the vicinity of the solute.

**Determination of Precise Terahertz Absorption Coefficients at 2.3–2.7 THz (75–90  $\text{cm}^{-1}$ ).** In addition, we have carried out THz absorption measurements of solvated urea using our p-Ge difference spectrometer.<sup>23</sup> High laser power in combination with a difference technique allows us to precisely determine THz absorption coefficients averaged over a frequency range between 2.3 and 2.7 THz. Figure 5 shows the absorption coefficient of aqueous urea solutions as a function of urea concentration at three different temperatures. In agreement with the wide band measurements, the average absorption increases with temperature. The starting slope as well as the

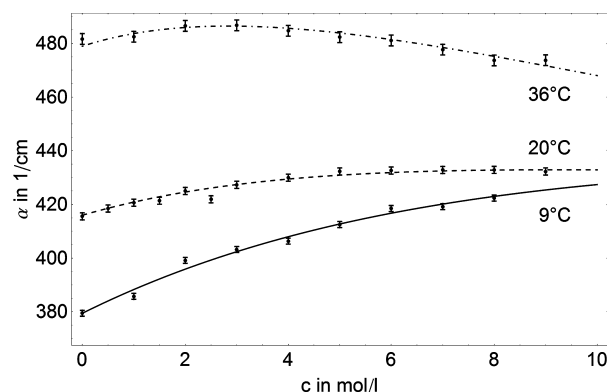


**Figure 5.** Displayed is the averaged THz absorption (between 2.3 and 2.7 THz) at fixed temperatures as a function of concentration for three different temperatures together with a simultaneous fit as described in the text.



difference between the absorption at low and high concentrations are strongly temperature dependent.

To summarize the findings of our experimental and simulation work of aqueous urea solutions, we find a temperature and concentration independent contribution to the THz absorption spectrum that may be attributed to translational and rotational rattling motions of weakly solvated urea in its surrounding water cage, a water contribution that increases with increasing temperature, and a small nonlinearity in the 2.3–2.7 THz range that may be attributed to vibrations of strongly solvated urea–water aggregates. Kaatz et al.<sup>33</sup> and Rezus and Bakker<sup>9</sup> found in their studies that the solvation shell of urea is composed of two types of water: one showing bulk like relaxation behavior and one forming longer lived solvated urea complexes. We modeled this behavior using a semi-ideal equilibrium approach (Methods) that treats the urea water system as an ideal mixture of weakly solvated urea monomer and urea water clusters of different size. The data sets for all three temperatures were fitted simultaneously with a total of seven parameters (Table 1) with the apparent molar volume of urea as determined by Gucker et al.<sup>34</sup>

**Table 1. Result of the Simultaneous Fit of Concentration Dependent THz Absorption at Three Different Temperatures; the Extinction of the Rattling Mode Was Determined As 20.2(7) l cm<sup>-1</sup> mol<sup>-1</sup>; the Values in Brackets Give the 95% Confidence Interval**

<i>T</i> in °C	<i>K</i> in cm <sup>3</sup> /mol <sup>a</sup>	<i>n</i> <sub>dilute</sub>	$\epsilon_{\text{shell}}(\tilde{\nu})$ in l cm <sup>-1</sup> mol <sup>-1</sup>	$\epsilon_{\text{bulk}}(\tilde{\nu})$ in l cm <sup>-1</sup> mol <sup>-1</sup>
9	6.01(58)	0.50	33(4)	6.84(2)
20	7.28(68)	0.68	25(2)	7.51(2)
36	9.39(86)	1.07	25(2) <sup>b</sup>	8.68(3)

<sup>a</sup>Calculated from  $\Delta G = 12.0(3)$  kJ/mol. <sup>b</sup>Identical to value for 20 °C.

The results of our fit are shown in Figure 5 and Table 1. The best fit is obtained with a free energy difference of  $\Delta G = 12.0(3)$  kJ/mol for the transition from weakly solvated urea to a urea–water complex. This yields association constants ranging from 6 to 9 cm<sup>3</sup>/mol and results in a very small average number

of water molecules bound to urea ranging from 0.5 water at 9 °C to 1.1 water at 36 °C. In agreement with our VDOS calculations, the urea–water complex extinction is larger than that of bulk water. The increased urea–water complex extinction at 9 °C compared to the higher temperature measurements is in full agreement with our broadband FTS data.

It is instructive to separate the three contributions to the total absorption according to eq 8: rattling by weakly solvated urea, THz excess due to urea–water complexes, and bulk water absorption as a function of concentration. This is done in the left part of Figure 6 for 9 °C (blue) and 36 °C (purple). The total absorption and experimental data are displayed as full line and dots, respectively. The dark and light shaded areas depict the THz excess due to urea–water clusters and rattling contributions, respectively. The unshaded areas below the dashed lines mark the expected water contribution to the total absorption assuming all water to behave bulklike (dilution effect). Bulk water dilution and its complexation with urea lead to a reduction in absorption. This effect is compensated by rattling mode and urea–water cluster absorption resulting in a nearly concentration independent total absorption coefficient.

Figure 6 (right) shows the mol fractions of urea strongly solvated by *n* water (top) and the mol fractions of water bound to urea in a urea–water complex containing *n* water (bottom). Although our model (Methods section) has no upper limit on *n*, the solvation shell is naturally limited by geometric progression. Only a small amount of solute is solvated by more than two water. According to our model, large urea concentrations lead to a shift in equilibria that reduces the amount of rigidly bound water in the solvation shell. Even at 10 M (urea/water = 1:3) concentration 80% of urea is not forming a strong urea water complex and the fraction of water in such complexes is on the order of a few percent. The observed nonlinearity in our absorption spectra is due to these shifted equilibria.

## DISCUSSION

Our wide band spectra indicate (Figure 1) that the total absorption of aqueous urea solutions can be described by a

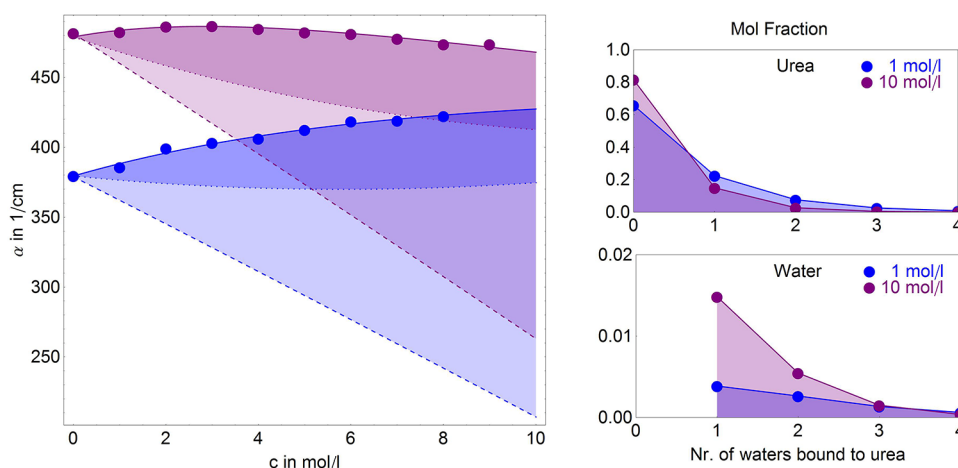


**Figure 6.** Left: Separation of the three contributions to total absorption (eq 8) for 9 °C (blue) and 36 °C (purple). The light and dark colored areas show the rattling contribution and the THz excess due to urea–water clusters, respectively. The dashed curves represent the bulk water absorption. Dots represent the experimental data. Right: Mol fractions of solutes strongly solvated by the given number of waters (top) and water bound to urea in a urea–water complex containing *n* water (bottom). Weakly solvated urea and urea bound to a single water dominate the distribution even at high solute concentration.

linear superposition of a temperature dependent water contribution and a temperature independent spectrum (e.g., Figure 2), which is linear as a function of concentration. If we use the more precise p-Ge difference spectrometer, a small nonlinearity is found (Figure 5). This indicates a small solvation shell in full agreement with Raman,<sup>35</sup> dielectric,<sup>33,36</sup> NMR,<sup>10</sup> and polarization-resolved mid-infrared pump–probe spectroscopy.<sup>9</sup> With increasing urea concentration bulk water absorption is reduced due to the dilution effect and urea–water complex formation. Nevertheless, the total absorption coefficient is nearly concentration independent because the sum of urea rattling and urea–water modes (Figure 6) compensates this effect. That this relationship holds over a wide frequency range indicates that both contributions show a very similar frequency spectrum. From the result of our MD simulations (Figure 3), both signals are likely due to intermolecular motions of urea and a urea–water cocluster within the water network.

The observed peaks at 100 and 150  $\text{cm}^{-1}$  can be compared to the results of previous optical Kerr effect measurements: The low frequency peak around 100  $\text{cm}^{-1}$  agrees very well with the absorption maximum, reported by Idrissi.<sup>17</sup> Idrissi et al. found the center frequency of this band to be temperature independent, in agreement with our findings. The band at 100  $\text{cm}^{-1}$  was previously assigned to a librational band of urea in the cage.<sup>17</sup> DFT calculations yielded a Raman active out of plane bending mode at 73  $\text{cm}^{-1}$  for urea–water and a mode at 99  $\text{cm}^{-1}$  for urea dimer.<sup>18</sup> In case of a band due to urea dimer formation, we would expect the leading term to depend on the square of the urea concentration. Instead, we find a mostly linear behavior. This points to an assignment to a urea rattling mode or urea–water cocluster vibrations.

Mazur et al.<sup>18</sup> reported a lower frequency 70–80  $\text{cm}^{-1}$  mode and a second mode at 150–175  $\text{cm}^{-1}$ , which were attributed to a rattling motion and to a water network mode, respectively. The redshift with increasing concentration of the 150  $\text{cm}^{-1}$  mode was interpreted as an indication of a disruption or distortion of the tetrahedral structure in liquid water. However, this is not in agreement with our results: We find a linear scaling with concentration for the absorption maximum but no shift in the center frequency when varying the concentration between 1 and 4 M (urea/water = 1:53 and 1:11, respectively).

Considering the fact that over a wide frequency range the spectrum of aqueous urea solution can be considered as a concentration weighted linear superposition of bulk water and urea rattling modes, we can only speculate that the frequency shift reported by Mazur might be caused by an incomplete model. For example, the red-shift of the 150  $\text{cm}^{-1}$  peak could be easily explained by a reduction in water contribution (at 175  $\text{cm}^{-1}$ ) and an increase in urea rattling mode strength (at 150  $\text{cm}^{-1}$ ) with increasing solute concentrations by our model without referring to a major change in the hydrogen bond network.

High precision THz absorption measurements using our p-Ge difference spectrometer were carried out to determine THz absorption coefficients and to deduce the free energy difference  $\Delta G = 12$  kJ/mol between the unbound and bound urea water states and the size of the dynamical hydration shell as a function of temperature. Our measurements favor a model where even at very high solute concentrations the majority of urea is only weakly hydrogen bonded to water and only few urea form strong solute–water complexes. This is in full agreement with Kaatz et al.<sup>33</sup> who distinguished between two kinds of water

molecules: one strongly bound to the urea and others that bind weakly. He derived 2–3 water molecules in the hydration shell of urea when focusing on slower motions recorded in the GHz range. Small dynamical hydration shells were also deduced from the results of dielectric measurements by Hayashi et al.<sup>36</sup> and by Rezus and Bakker.<sup>9</sup>

Rezus and Bakker proposed a solvation structure where water singly hydrogen bonded to urea show fast bulklike relaxation, whereas water doubly hydrogen bonded to urea are highly immobilized. Following this line, our semi-ideal model describes urea–water aggregation by formation of a second hydrogen bond. An attempt to fit both  $\Delta H$  and  $\Delta S$  from our data yielded  $\Delta H = 5.5$  kJ/mol and  $\Delta S = -23$  J mol<sup>-1</sup> K<sup>-1</sup> with large uncertainties. Thus, we estimate that about half of the change in free energy is due to enthalpic effects. Interestingly, Stumpe and Grubmüller predict a change in H-bond energy of  $\approx 5$  kJ/mol when replacing a water oxygen as hydrogen bond acceptor by urea oxygen and  $\sim 10$  kJ/mol when replacing water oxygen as hydrogen bond donor by urea nitrogen. This is a strong indication that the spectral changes we observe are due to water immobilization by double hydrogen bond formation.

Up to concentrations of 4 M we find no indication for aggregation of urea, which should result in a deviation from linearity or a frequency shift of the rattling peaks due to a change in the environment, although urea aggregation was proposed to take place at concentrations beyond 6 M by Stumpe and Grubmüller.<sup>37</sup>

In summary, we find that the influence of urea on the water network is weak; urea seems to fit nearly perfectly into the water network. The observed low frequency modes of the partial solute THz absorption agree well with the predicted VDOS attributed to the rotational and translational motions of the solvated urea itself. The dynamical hydration shell size is found to be small. We find no indication of a long-range effect on the hydration bond dynamics. Our experimental results do not support a classification of urea as a structure breaker; instead we find that urea and water are readily interchangeable. These findings support a direct rather than an indirect mechanism of the denaturation by urea.

## METHODS

**Broadband Fourier Transform Terahertz Spectroscopy.** We recorded the concentration dependent THz spectra of urea in the frequency range from 50–400  $\text{cm}^{-1}$  using a Bruker 80 Vertex spectrometer with a helium-cooled bolometer as detector and a silicon carbide lamp as light source. The sample chamber was purged with liquid nitrogen. Standard Bruker liquid cells equipped with 500  $\mu\text{m}$  CVD diamond windows served as sample holders. The optical path length in the sample cell was fixed by PTFE spacers to 40  $\mu\text{m}$ . The thickness of the cell was determined by measuring the frequency spacing between subsequent etalons in an empty cell.

For the determination of the absorption coefficient the following procedure was used:

1. The absolute absorption  $\alpha_{w,0^\circ\text{C}}$  of the water sample kept at 0  $^\circ\text{C}$  was determined for two spacing sizes, that is two different path lengths. Note, that at 0  $^\circ\text{C}$ , the absorption is decreased compared to room temperature, allowing for larger path lengths.
2. The difference  $\Delta\alpha_{w,0^\circ\text{C};T}$  between the THz absorption of water at 0  $^\circ\text{C}$  and water at the designated temperature  $T$

(in our case 9, 20, or 36 °C) was determined. Here, we used a spacer thickness of 40  $\mu\text{m}$ .

3. The difference in THz absorption  $\Delta\alpha_{s,T}$  between the sample and water was measured using a fixed spacer size. The temperature  $T$  was kept constant with an accuracy of 0.5 °C. The absolute absorption coefficient was then calculated according to:

$$\alpha_{s,T} = \alpha_{w,0^\circ\text{C}} + \Delta\alpha_{w,0^\circ\text{C};T} + \Delta\alpha_{s,T} \quad (2)$$

**Molecular Dynamics Simulations.** To get a deeper insight into the molecular details of solvation, we have carried out molecular dynamics (MD) simulations of solvated urea using the program package GROMACS 3.3.<sup>27</sup> The simulation protocol is described in detail by Oostenbrink et al.<sup>38</sup> The GROMOS force field 53a5 was used for a description of the potential energy of urea, and the SPC force field for water.<sup>38,39</sup> The simulated system consisted of 56 urea molecules, randomly distributed in a cubic box (with an edge length of 47.4 Å) solvated by 4145 water molecules. We used periodic boundary conditions. The system was relaxed and afterward preequilibrated for 25 ps using an NVT ensemble at 300 K with a Berendsen thermostat<sup>39</sup> and a time constant of 0.1 ps, while restraining the positions of the urea molecules. Next, we performed an equilibration in the NPT ensemble for 50 ps. We used the Berendsen barostat with a time constant of 0.5 ps at a reference pressure of 1 bar with a compressibility of  $4.5 \times 10^{-5} \text{ bar}^{-1}$ . The box length relaxed to 51.10 Å during the simulation. In the next step, we extended the simulation for 2 ns to take every 100 ps snapshots as starting points for NVE simulations of 20 ps length. Upon the basis of the NVE simulations, we have calculated the vibrational density of states of the urea molecules. The coordinates of the NVE simulation were saved every 2 fs. The computation of the long-range electrostatic interactions was realized via the Particle-Mesh Ewald method with a Fourier spacing of 1.2 Å.<sup>40</sup> For the short-ranged interactions as well as for the LJ interactions the cut off radius was set to 10 Å.

**Measurement of Precise THz Absorption Coefficients.** Integrated THz absorption measurements in the frequency range from 2.1 to 2.8 THz were recorded using our p-Ge difference spectrometer as described previously.<sup>23</sup> We used a double-beam configuration for background subtraction. Two mirror-choppers with a rotational frequency of 60 Hz are synchronized to the laser pulse train and direct the laser beam subsequently through the sample and the reference cell. For each data point 30 000 pulses were averaged. The change in the absorption coefficient is a measure of the changes in the collective water network vibrations induced by urea. To determine the absorption coefficient of the sample and the reference, the transmitted THz radiation of both channels are measured subsequently. By Beer's law, we determined  $\Delta\alpha$  as the difference of the average THz absorbance of the sample solution ( $\alpha_{\text{sample}}$ ) and of the water reference ( $\alpha_{\text{reference}}$ ) between 2.4 and 2.7 THz:  $\Delta\alpha = \alpha_{\text{sample}} - \alpha_{\text{reference}}$ . THz absorbance measurements were performed at low-humidity (<8%). Both cells were kept simultaneously under temperature stabilized conditions ( $T \pm 0.05 \text{ K}$ , where  $T$  is the respective experimental temperature). In a second step, we used the sample cell, which was then filled with water, and measured the transmitted THz radiation in this configuration to determine the absolute absorption coefficients.

**Semi-Ideal Aggregation Model.** We have used a semi-ideal equilibrium model, which is similar to that used for sugars by Stokes and Robinson.<sup>41</sup> Shortly, the formation of solute–water complexes is described by an infinite series of association reactions of the form



where  $S_n$  describes a solute–water complex containing  $n$  water molecules and  $K_n$  gives the corresponding association constant for changing the number of waters in the complex from  $(n - 1)$  to  $n$ . Because of the lack of a priori knowledge and to minimize the number of adjustable parameters (Ockham's razor), we put no upper limit to  $n$ . Thus, in principle our model also takes into account cooperativity, that is a locally extended solvation shell similar to that found in sugars and proteins.<sup>21,22,42</sup> Upon the basis of the small nonlinearity in our p-Ge measurements, we expect a small solvation shell size. Therefore, we assume for simplicity, that  $K_n = K$  for all  $n$ . With this approximation, the concentration of a solute bound to  $n$  solvent molecules is given by

$$[S_n] = K^n [S][\text{H}_2\text{O}]^n \quad (4)$$

where  $[S]$  is the concentration of weakly solvated solute and  $[\text{H}_2\text{O}]$  the concentration of unbound water. After evaluation of the corresponding infinite sums, the known concentrations  $c_s$  and  $c_w = (1/V_0)(1 - c_s\phi)$  of solute and solvent respectively pose the following two boundary conditions on the system:

$$\frac{[S]}{1 - K[\text{H}_2\text{O}]} = c_s \quad (5)$$

$$\frac{c_s K [\text{H}_2\text{O}]}{1 - K[\text{H}_2\text{O}]} + [\text{H}_2\text{O}] = \frac{1}{V_0}(1 - c_s\phi) \quad (6)$$

where  $V_0$  and  $\phi$  are the molar volume of bulk water and the apparent molar volume of the solute, respectively. The latter equation may be solved analytically or numerically for  $[\text{H}_2\text{O}]$ . A closer inspection shows that the expectation value of the number of water molecules strongly bound to the solute is given by

$$n_{\text{shell}}(c_s) = \frac{K[\text{H}_2\text{O}]}{1 - K[\text{H}_2\text{O}]} \quad (7)$$

Eq 7 reduces to  $n_{\text{dilute}} = K/(V_0 - K)$  for dilute solutions.  $n_{\text{shell}}$  is concentration dependent due to the shift in equilibria.

To be able to connect this chemical model to spectral observations, we assume in addition that the effective extinction spectra of the weakly solvated solute ( $\epsilon_{\text{rattling}}$ ), the unbound and weakly solvating water ( $\epsilon_{\text{bulk}}$ ), and the solute–water complexes ( $\epsilon_{\text{solv}}$ ) do not depend on the solute concentration. We further assume that the weakly solvating water shows a bulklike absorption spectrum. For solute–water complexes we expect that – due to coupling to the thermal bath of the surrounding water – the shape of the extinction curve is independent of the number  $n$  of strongly attached water, that its intensity, however, is proportional to  $n$ . This is reasonable in case of intramolecular modes since for example a urea water cluster containing two water should show two urea water stretch vibrations closely spaced or even degenerate in frequency. These assumptions lead to a total THz absorption that is described by



$$\alpha(c_s, T) = c_s(1 - K(T)[\text{H}_2\text{O}])\epsilon_{\text{rattling}} + c_s \frac{K(T)[\text{H}_2\text{O}]}{1 - K(T)[\text{H}_2\text{O}]}(\epsilon_{\text{solv}} - \epsilon_{\text{bulk}}) + \frac{1}{V_0}(1 - c_s\phi)\epsilon_{\text{bulk}} \quad (8)$$

that is a linear superposition of a rattling contribution ( $\epsilon_{\text{rattling}}$ ), the difference (THz excess) between solute–solvent complex and bulk extinction ( $\epsilon_{\text{solv}} - \epsilon_{\text{bulk}}$ ), and a bulk contribution ( $\epsilon_{\text{bulk}}$ ), respectively. To reduce the number of parameters, we used the form  $K(T) = e^{-(\Delta G)/(RT)}$  with  $R$ ,  $\Delta G$ , and  $T$  as molar gas constant, change in free energy, and temperature, respectively. A fit of the experimental concentration dependent data gives therefore access to  $\Delta G$ .

## AUTHOR INFORMATION

### Corresponding Author

\*E-mail: gerhard.schwaab@rub.de.

### Notes

The authors declare no competing financial interest.

## ACKNOWLEDGMENTS

The authors thank E.Bründermann, G.Niehues and M. Heyden for fruitful discussions and scientific support. The FT spectrometer was provided by BMBF grant 05 KS7PC2.

## REFERENCES

- (1) Frank, H. S.; Franks, F. *J. Chem. Phys.* **1968**, *48*, 4746–4757.
- (2) Franks, F. *Biophys. Chem.* **2002**, *96*, 117–127.
- (3) Finer, E. G.; Franks, F.; Tait, M. J. *J. Am. Chem. Soc.* **1972**, *94*, 4424–4429.
- (4) Idrissi, A.; Cinar, E.; Longelin, S.; Damay, P. *J. Mol. Liq.* **2004**, *110*, 201–208.
- (5) Walrafen, G. E. *J. Chem. Phys.* **1966**, *44*, 3726–3727.
- (6) Idrissi, A.; Gerard, M.; Damay, P.; Kiselev, M.; Puhovsky, Y.; Cinar, E.; Lagant, P.; Vergoten, G. *J. Phys. Chem. B* **2010**, *114*, 4731–4738.
- (7) Rupley, J. A. *J. Phys. Chem.* **1964**, *68*, 2002–2003.
- (8) Herskovits, T. T.; Kelly, T. M. *J. Phys. Chem.* **1973**, *77*, 381–388.
- (9) Rezus, Y. L. A.; Bakker, H. J. *Proc. Natl. Acad. Sci. U. S. A.* **2006**, *103*, 18417–18420.
- (10) Shimizu, A.; Fumino, K.; Yukiya, K.; Taniguchi, Y. *J. Mol. Liq.* **2000**, *85*, 269–278.
- (11) Turner, J.; Finney, J.; Soper, A. *Zeitschrift für Naturforschung A: Physical Sciences* **1991**, *46*, 73–83.
- (12) Hua, L.; Zhou, R.; Thirumalai, D.; Berne, B. J. *Proc. Natl. Acad. Sci. U. S. A.* **2008**, *105*, 16928–16933.
- (13) Whittington, S. J.; Chellgren, B. W.; Hermann, V. M.; Creamer, T. P. *Biochemistry* **2005**, *44*, 6269–6275.
- (14) Soper, A.; E., C., Jr.; Luzar, A. *Biophys. Chem.* **2003**, *105*, 649–666.
- (15) Stumpe, M. C.; Grubmüller, H. *Biophys. J.* **2009**, *96*, 3744–3752.
- (16) Canchi, D. R.; Paschek, D.; García, A. E. *J. Am. Chem. Soc.* **2010**, *132*, 2338–2344.
- (17) Idrissi, A.; Bartolini, P.; Ricci, M.; Righini, R. *Phys. Chem. Chem. Phys.* **2003**, *5*, 4666–4671.
- (18) Mazur, K.; Heisler, I. A.; Meech, S. R. *J. Phys. Chem. B* **2011**, *115*, 2563–2573.
- (19) Schmidt, D. A.; Birer, O.; Funkner, S.; Born, B. P.; Gnanasekaran, R.; Schwaab, G. W.; Leitner, D. M.; Havenith, M. *J. Am. Chem. Soc.* **2009**, *131*, 18512–18517.
- (20) Funkner, S.; Niehues, G.; Schmidt, D. A.; Heyden, M.; Schwaab, G.; Callahan, K. M.; Tobias, D. J.; Havenith, M. *J. Am. Chem. Soc.* **2012**, *134*, 1030–1035.
- (21) Heyden, M.; Bründermann, E.; Heugen, U.; Niehues, G.; Leitner, D. M.; Havenith, M. *J. Am. Chem. Soc.* **2008**, *130*, 5773–5779 PMID: 18393415.
- (22) Heugen, U.; Schwaab, G.; Bründermann, E.; Heyden, M.; Yu, X.; Leitner, D. M.; Havenith, M. *Proc. Natl. Acad. Sci. U. S. A.* **2006**, *103*, 12301–12306.
- (23) Bergner, A.; Heugen, U.; Bründermann, E.; Schwaab, G.; Havenith, M.; Chamberlin, D. R.; Haller, E. E. *Rev. Sci. Instrum.* **2005**, *76*, 063110.
- (24) Zelsmann, H. R. *J. Mol. Struct.* **1995**, *350*, 95–114.
- (25) Bertie, J. E.; Lan, Z. *Appl. Spectrosc.* **1996**, *50*, 1047–1057.
- (26) Heyden, M.; Sun, J.; Funkner, S.; Mathias, G.; Forbert, H.; Havenith, M.; Marx, D. *Proc. Natl. Acad. Sci. U. S. A.* **2010**, *107*, 12068–12073.
- (27) Van Der Spoel, D.; Lindahl, E.; Hess, B.; Groenhof, G.; Mark, A. E.; Berendsen, H. J. C. *J. Comput. Chem.* **2005**, *26*, 1701–1718.
- (28) Li, Y.; Lin, S.-T.; Goddard, W. A. *J. Am. Chem. Soc.* **2004**, *126*, 1872–1885, PMID: 14871120.
- (29) Louck, J. D.; Galbraith, H. W. *Rev. Mod. Phys.* **1976**, *48*, 69–106.
- (30) Janežič, D.; Praprotnik, M.; Merzel, F. *J. Chem. Phys.* **2005**, *122*, 174101.
- (31) Brown, R.; Godfrey, P.; Storey, J. *J. Mol. Spectrosc.* **1975**, *58*, 445–450.
- (32) Vijay, A.; Sathyanarayana, D. *J. Mol. Struct.* **1993**, *295*, 245–258.
- (33) Kaatz, U.; Gerke, H.; Pottel, R. *J. Phys. Chem.* **1986**, *90*, 5464–5469.
- (34) Gucker, F. T.; Gage, F. W.; Moser, C. E. *J. Am. Chem. Soc.* **1938**, *60*, 2582–2588.
- (35) Hockett, X.; Turrell, G. *J. Chem. Phys.* **1993**, *99*, 8498.
- (36) Hayashi, Y.; Katsumoto, Y.; Omori, S.; Kishii, N.; Yasuda, A. *J. Phys. Chem. B* **2007**, *111*, 1076–1080.
- (37) Stumpe, M. C.; Grubmüller, H. *J. Phys. Chem. B* **2007**, *111*, 6220–6228.
- (38) Oostenbrink, C.; Villa, A.; Mark, A. E.; Van Gunsteren, W. F. *J. Comput. Chem.* **2004**, *25*, 1656–1676.
- (39) Berendsen, H. J. C.; Postma, J. P. M.; van Gunsteren, W. F.; DiNola, A.; Haak, J. R. *J. Chem. Phys.* **1984**, *81*, 3684–3690.
- (40) Darden, T.; York, D.; Pedersen, L. *J. Chem. Phys.* **1993**, *98*, 10089–10092.
- (41) Stokes, R. H.; Robinson, R. A. *J. Phys. Chem.* **1966**, *70*, 2126–2131.
- (42) Ebbinghaus, S.; Kim, S. J.; Heyden, M.; Yu, X.; Gruebele, M.; Leitner, D. M.; Havenith, M. *J. Am. Chem. Soc.* **2008**, *130*, 2374–2375.